Cross-Scale Internal Graph Neural Network for Image Super-Resolution

(Supplementary Materials)

Shangchen Zhou[1] **Jiawei Zhang**[2] **Wangmeng Zuo**[3] **Chen Change Loy**[1]*
[1]Nanyang Technological University [2]SenseTime Research [3]Harbin Institute of Technology
{s200094,ccloy}@ntu.edu.sg zhangjiawei@sensetime.com wmzuo@hit.edu.cn
https://github.com/sczhou/IGNN

In this supplementary material, we provide additional details and results to the paper. In Sec. A, we first present the detailed architectures of two small sub-networks in the proposed Graph Aggregation module (GraphAgg). Then, we give an illustration of operation details in the GraphAgg. Sec. B presents further analysis and discussions on our proposed GraphAgg module and IGNN network. Finally, we show more visual experimental results compared with other state-of-the-art SR networks in Sec. C.

A Details in GraphAgg

A.1 Architecture Details

As presented in Sec. 2.2 in the manuscript, the proposed GraphAgg has two small sub-networks: Edge-Conditioned sub-network (ECN) and Downsampled-Embedding sub-network (DEN). Tables 1 and 2 list the detailed configurations of ECN and DEN, respectively. In Graph Construction, we use the first three layers of the VGG19 [5] with fixed pre-trained parameters.

Table 1: Architecture of the Edge-Conditioned sub-network (ECN).

Layer	Kernel	Stride	Padding	Feature
Input ($\mathcal{D}^{n_r \to q}$)				64
Conv/ReLU	1×1	1	1	64
Conv/ReLU	1×1	1	1	64
Conv	1×1	1	1	1

Table 2: Architecture of the Downsampled-Embedding sub-network (DEN).

Layer	Kernel	Stride	Padding	Feature
Input ($F_{L\uparrow s}$)				256
Conv/ReLU	5×5	1	1	256
Conv/ReLU	3×3	1	1	256
Conv	3×3	1	1	256

A.2 Illustration of Detailed Processes in GraphAgg

To further clarify the operations in the GraphAgg, we illustrate the details as shown in Figure 1.

In Figure 1(a), we extract $l \times l$ LR patches using *img2patch* operation with a stride of g from features $E_{L\downarrow s}$ and E_L, where we set $l = 3$ and $g = 2$ in our network. Thus we obtain $m_1 \times n_1$ LR patches (denoted as $\mathcal{V}_1^l$) and $m_2 \times n_2$ LR patches (denoted as $\mathcal{V}_2^l$) from $E_{L\downarrow s}$ and E_L respectively. Denote the feature shapes of $E_{L\downarrow s}$ and E_L as $H/s \times W/s$ and $H \times W$ respectively. Therefore, $m_1 = \lfloor (H/s - l)/g \rfloor + 1, n_1 = \lfloor (W/s - l)/g \rfloor + 1$, and $m_2 = \lfloor (H - l)/g \rfloor + 1, n_2 = \lfloor (W - l)/g \rfloor + 1$. Each LR patch in $\mathcal{V}_2^l$ find the k nearest neighboring LR patches from $\mathcal{V}_1^l$ according to the Euclidean distance. Note that we do not consider the searching window in this discussion for simplicity.

To obtain k corresponding HR ($ls \times ls$) patch regions in E_L scale, we map each LR patch in $E_{L\downarrow s}$ to HR regions in E_L scale, as shown in Figure 1(b). In E_L scale, the $ls \times ls$ patch regions are obtained

*Corresponding Author.

34th Conference on Neural Information Processing Systems (NeurIPS 2020), Vancouver, Canada.

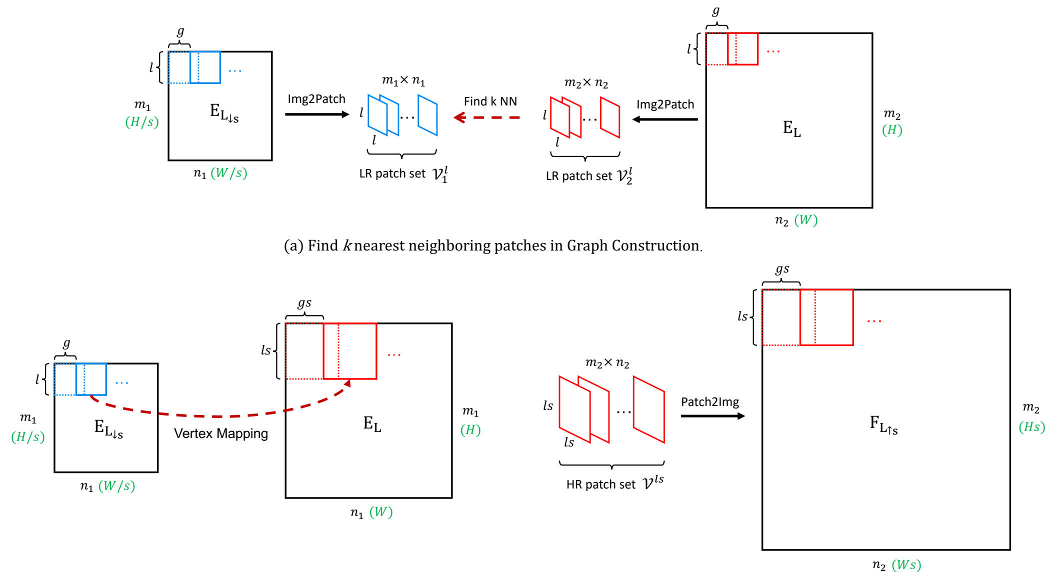

(a) Find k nearest neighboring patches in Graph Construction.

(b) Vertex Mapping in Graph Construction.

(c) Patch2Img in Patch Aggregation.

Figure 1: In (a), $n_1 \times m_1$ LR patches and $n_2 \times m_2$ LR patches are extracted using *img2patch* operation with a stride of g from features $E_{L\downarrow s}$ and E_L, respectively. Each LR patch of E_L find the k nearest neighboring LR patches from $E_{L\downarrow s}$. In (b), each found LR patch in $E_{L\downarrow s}$ is mapped to a HR region in E_L scale. In E_L scale, the HR patch regions are extracted using *img2patch* operation with the stride of gs. In (c), we transform $n_2 \times m_2$ HR patches to the final HR feature $F_{L\uparrow s}$ using a *patch2img* operation with the stride of gs. Note that the sizes of LR and HR patches are $l \times l$ and $ls \times ls$, respectively, where s is desired upsampling factor. Refer to Sec. A.2 for more details.

using *img2patch* operation with the stride of gs. It exactly has the same number $(m_1 \times n_1)$ of patches as LR patches in $E_{L\downarrow s}$, i.e., $\lfloor (H - ls)/gs \rfloor + 1 = m_1$, $\lfloor (W - ls)/gs \rfloor + 1 = n_1$. Therefore, the LR and HR patch regions from $E_{L\downarrow s}$ and E_L scales can be matched one-on-one.

As presented in Eq. (2) in the manuscript, we obtain one aggregated HR patch for each LR patch in the LR patch set $\mathcal{V}_2^l$, which contains $m_2 \times n_2$ LR patches. Thus, we obtain a HR patch set $\mathcal{V}^{rs}$ containing $m_2 \times n_2$ HR patches with $ls \times ls$ patch size. Figure 1(c) shows that we take the $\mathcal{V}^{rs}$ as input and use a *patch2img* operation with the stride of gs to generate the HR features $F_{L\uparrow s}$.

B More Discussions on GraphAgg and IGNN

In this section, we first present more ablation experiments to demonstrate the effectiveness of the proposed IGNN further, including the effect of using F'_L and $F_{L\uparrow s}$ and number of GraphAgg modules inserted in networks. In addition, we report and compare the runtime of the state-of-the-art networks and the proposed IGNN.

B.1 Effectiveness of F'_L and $F_{L\uparrow s}$

To validate the effectiveness of both enriched features F'_L and aggregated HR features $F_{L\uparrow s}$, we compare our network with three variant networks: replacing the enriched LR features F'_L by the original LR features F_L (w/o F'_L), removing aggregated HR features $F_{L\uparrow s}$ (w/o $F_{L\uparrow s}$) and without both of them (baseline), i.e., EDSR. According to Table 3, these three variant networks generate worse SR results compared to the completed network.

B.2 Effectiveness of of Multiple GraphAgg Module

To explore whether the number of GraphAgg module affects IGNN performance, we evaluate to insert 1 (after 16th residual block), 2 (after 8th and 24th residual block), and 3 (after 8th, 16th, and 24th residual block) GraphAgg modules in the backbone network, respectively. As shown in Table 4, using more GraphAgg module only leads to slight PSNR/SSIM gains. Thus we only employ one

Table 3: Results on Urban100 ($\times 2$) for different variants of networks. The (w/o F'_L) represents replacing the enriched LR features F'_L by the original LR features F_L, and (w/o $F_{L\uparrow s}$) represents removing the aggregated HR features $F_{L\uparrow s}$. Note the EDSR is our baseline which is equivalent to removing both F'_L and $F_{L\uparrow s}$.

	baseline (EDSR)	w/o F'_L	w/o $F_{L\uparrow s}$	IGNN
PSNR	32.93	33.19	33.13	**33.23**
SSIM	0.9351	0.9379	0.9374	**0.9383**

GraphAgg module in our IGNN as a trade-off among the computational complexity and performance. Compared with the baseline network (EDSR) without GraphAgg inserted, our proposed IGNN shows a large performance gain.

Table 4: Results on Urban100 ($\times 2$) for different numbers of GraphAgg modules are inserted in the networks.

	0 (baseline)	**1 (after 16th)**	2 (after 8th and 24th)	3 (after 8th, 16th, and 24th)
PSNR	32.93	33.23	33.23	33.25
SSIM	0.9351	0.9383	0.9384	0.9385

B.3 Relationship between Performance Gain and Self-similarity Level

It is worth to analyze further on performance gains for different self-similarity levels. As shown in Figure 2, our method performs better in regions with self-similarity, especially in regions where texture patterns are extremely small. Besides, the performance can also be well maintained to that of EDSR in regions with few self-similar patches.

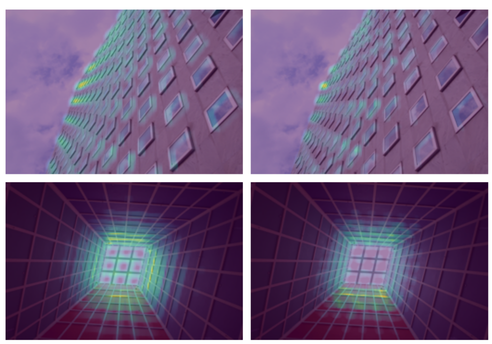

Self-similarity Level PSNR Gain

Figure 2: Examples to show the relationship between self-similarity level and PSNR gain (over EDSR). The brighter regions indicate larger values.

B.4 Runtime

Here, we report and compare the runtime of state-of-the-art networks [8, 4, 7, 2, 1] and the proposed IGNN. All existing methods are evaluated using their publicly available code. As shown in Table 5, the proposed network has comparable runtime as [8, 4, 7, 2], but it has better performance on all benchmarks at all scales (Refer to Table 1 in the manuscript). As for SAN [1], the proposed IGNN runs over two times faster than it, and performs better in most cases.

Table 5: Runtime of different networks. All methods are evaluated on an NVIDIA Tesla V100 GPU.

	RDN [8]	EDSR [4]	RNAN [7]	OISR-RK3 [2]	SAN [1]	IGNN (Ours)
PSNR	32.89	32.93	32.73	33.03	33.10	**33.23**
Time (sec)	1.538	1.416	2.280	1.833	5.971	2.676

C Qualitative Comparisons

In this section, we provide more visual comparisons with seven state-of-the-art SISR networks, i.e., VDSR [3], EDSR [4], RDN [8], RCAN [6], OISR [2], SAN [1], and RNAN [7], on standard benchmark datasets. As shown in Figure 3 and Figure 4, the proposed IGNN recovers richer and sharper details from the LR images especially in the regions with recurring patterns.

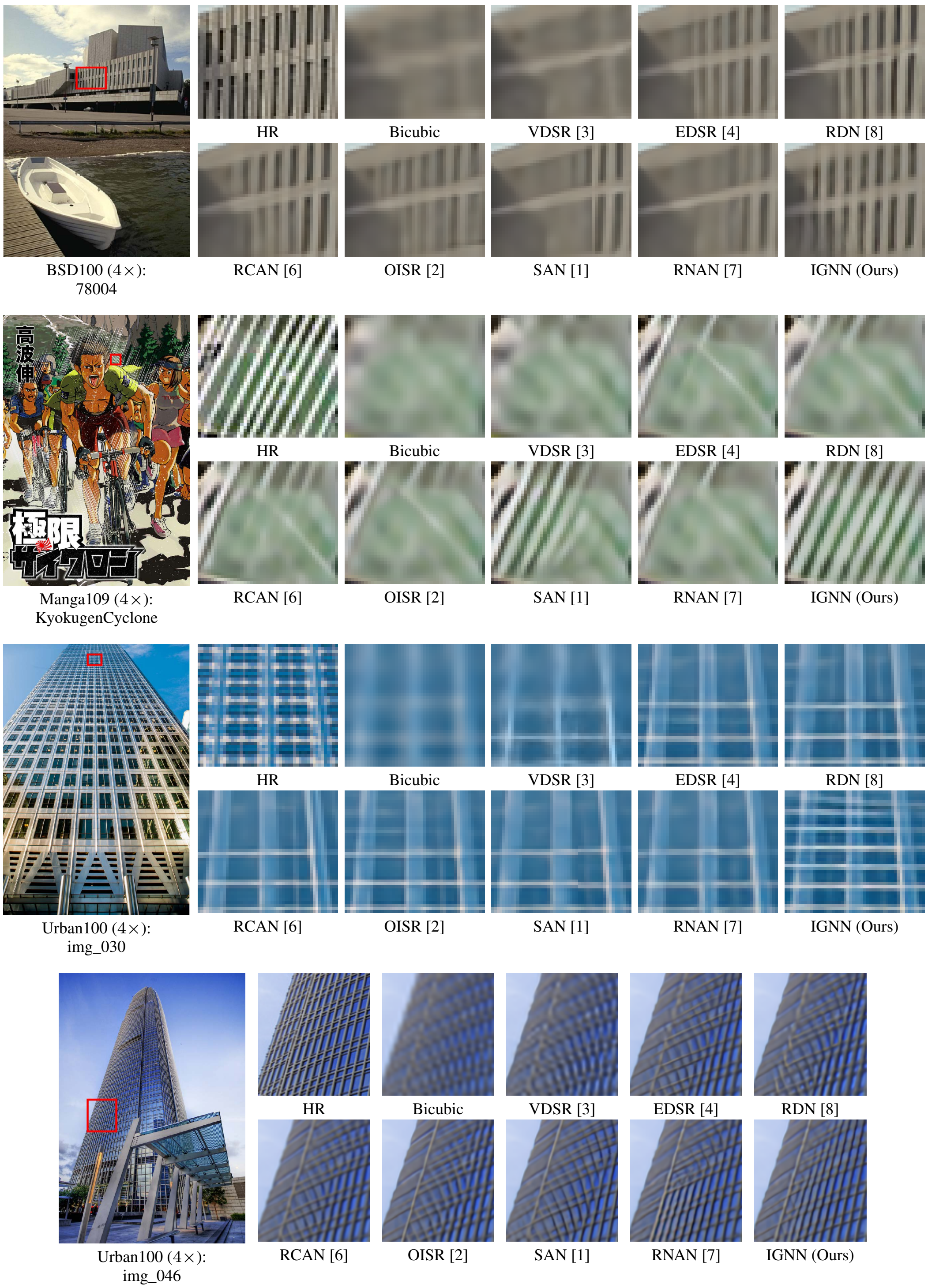

Figure 3: Visual comparison for $\times 4$ SR on benchmark datasets.

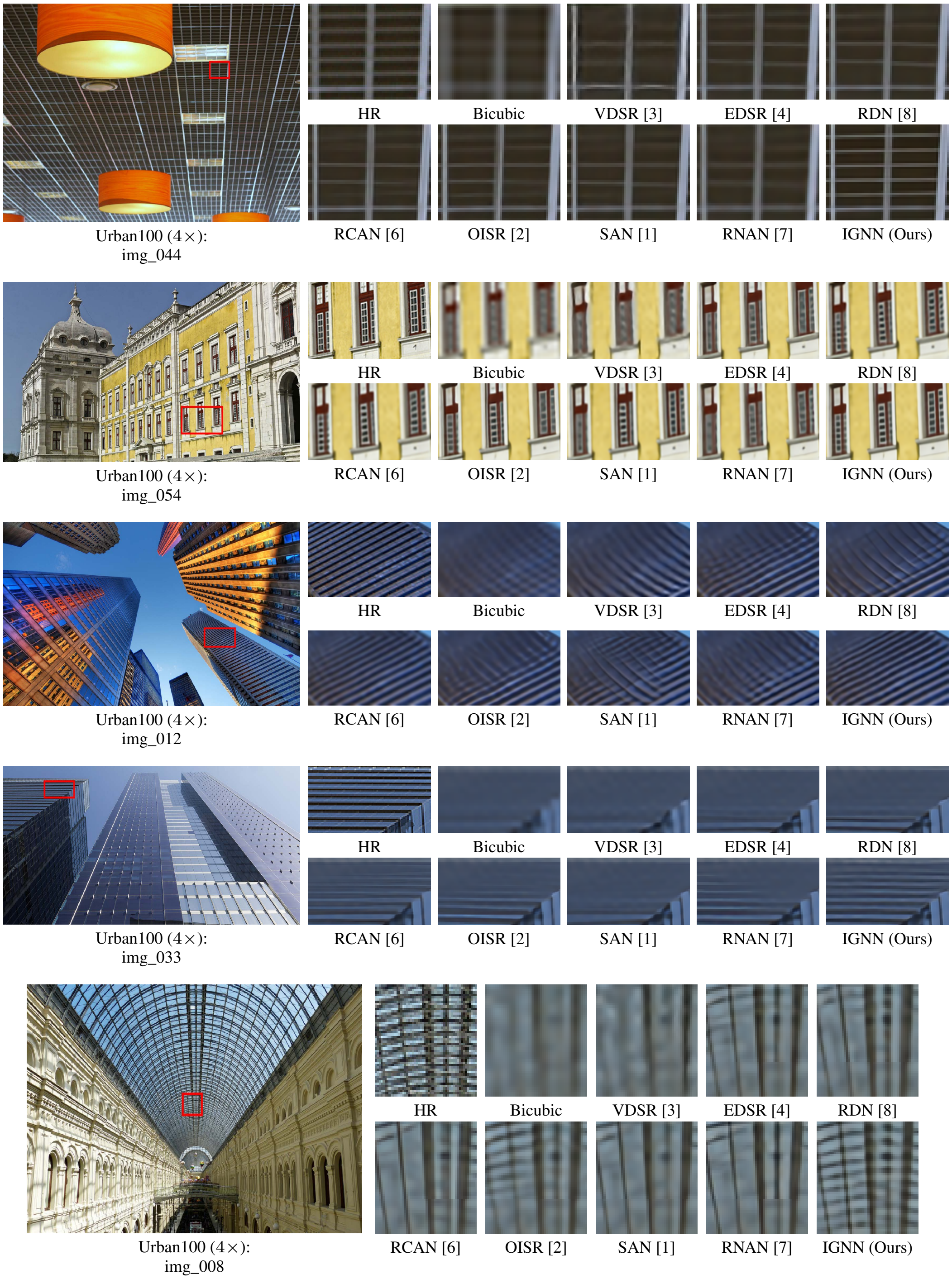

Figure 4: Visual comparison for $\times 4$ SR on benchmark datasets.

References

[1] Tao Dai, Jianrui Cai, Yongbing Zhang, Shu-Tao Xia, and Lei Zhang. Second-order attention network for single image super-resolution. In *CVPR*, 2019.

[2] Xiangyu He, Zitao Mo, Peisong Wang, Yang Liu, Mingyuan Yang, and Jian Cheng. Ode-inspired network design for single image super-resolution. In *CVPR*, 2019.

[3] Jiwon Kim, Jung Kwon Lee, and Kyoung Mu Lee. Accurate image super-resolution using very deep convolutional networks. In *CVPR*, 2016.

[4] Bee Lim, Sanghyun Son, Heewon Kim, Seungjun Nah, and Kyoung Mu Lee. Enhanced deep residual networks for single image super-resolution. In *CVPRW*, 2017.

[5] Karen Simonyan and Andrew Zisserman. Very deep convolutional networks for large-scale image recognition. *arXiv preprint arXiv:1409.1556*, 2014.

[6] Yulun Zhang, Kunpeng Li, Kai Li, Lichen Wang, Bineng Zhong, and Yun Fu. Image super-resolution using very deep residual channel attention networks. In *ECCV*, 2018.

[7] Yulun Zhang, Kunpeng Li, Kai Li, Bineng Zhong, and Yun Fu. Residual non-local attention networks for image restoration. In *ICLR*, 2019.

[8] Yulun Zhang, Yapeng Tian, Yu Kong, Bineng Zhong, and Yun Fu. Residual dense network for image super-resolution. In *CVPR*, 2018.